

**CHARACTERISATION OF HEAT AND MASS
TRANSFER IN THE RECTANGULAR FLAT-
SHEET POLYVINYLIDENE FLUORIDE
MEMBRANE FOR VACUUM MEMBRANE
DISTILLATION**

CHIAM CHEL KEN



UMS
PERPUSTAKAAN
UNIVERSITI MALAYSIA SABAH

**THESIS SUBMITTED IN FULLFILMENT FOR
THE DEGREE OF DOCTOR OF PHILOSOPHY**

**FACULTY OF ENGINEERING
UNIVERSITI MALAYSIA SABAH
2014**

UNIVERSITI MALAYSIA SABAH

BORANG PENGESAHAN STATUS TESIS

JUDUL : CHARACTERISATION OF HEAT AND MASS TRANSFER IN THE RECTANGULAR FLAT-SHEET POLYVINYLIDENE FLUORIDE MEMBRANE FOR VACUUM MEMBRANE DISTILLATION

IJAZAH : DOKTOR FALSAFAH (KEJURUTERAAN KIMIA)

SAYA **CHIAM CHEL KEN** SESI PENGAJIAN: **2010 – 2014**
mengaku membenarkan tesis (Doktor Falsafah) ini disimpan di Perpustakaan Universiti Malaysia Sabah dengan syarat-syarat kegunaan seperti berikut: -

1. Tesis adalah hakmilik Universiti Malaysia Sabah
2. Perpustakaan Universiti Malaysia Sabah dibenarkan membuat salinan untuk tujuan pengajian sahaja
3. Perpustakaan dibenarkan membuat salinan tesis ini sebagai bahan pertukaran antara institusi pengajian tinggi
4. Sila tandakan (✓)

SULIT

(Mengandungi maklumat berdarjah keselamatan dan kepentingan Malaysia seperti yang termaktub di AKTA RAHSIA 1972)

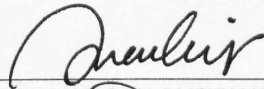
TERHAD

(Mengandungi maklumat TERHAD yang telah ditentukan oleh organisasi/badan di mana penyelidikan dijalankan)

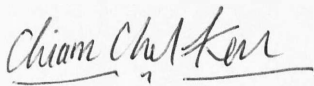
TIDAK TERHAD

NURULAIN BINTI ISMAIL
Disahkan oleh
LIBRARIAN

UNIVERSITI MALAYSIA SABAH




(TANDATANGAN PUSTAKAWAN)



(TANDATANGAN PENULIS)

Tarikh: 23 Jun 2014



PROF. IR. DR. ROSALAM HJ. SARBATLY

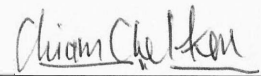
Tarikh: 23 Jun 2014

DECLARATION

I hereby declare that the data of the research written in this thesis are original and the experimental data are found by me. This thesis has not been submitted previously for a higher degree in any university.

In addition, I also declare that the material in this thesis is my own except for quotations, excerpts, equations, summaries and references, which have been duly acknowledged.

25 June 2014



Chiam Chel Ken

PK2009 9075



UMS
UNIVERSITI MALAYSIA SABAH

CERTIFICATION

NAME : **CHIAM CHEL KEN**
MATRIC NO. : **PK2009 9075**
TITLE : **CHARACTERISATION OF HEAT AND MASS TRANSFER
IN THE RECTANGULAR FLAT-SHEET POLYVINYLIDENE
FLUORIDE MEMBRANE FOR VACUUM MEMBRANE
DISTILLATION**
DEGREE : **DOCTOR OF PHILOSOPHY (CHEMICAL ENGINEERING)**
VIVA DATA : **12 MARCH 2014**



1. SUPERVISOR

Prof. Ir. Dr. Rosalam Hj. Sarbatly

DECLARED BY

UMS
UNIVERSITI MALAYSIA SABAH

Signature

A handwritten signature in black ink, appearing to read 'R. Sarbatly', written over a horizontal line.

ACKNOWLEDGEMENT

I want to give thanks to my God, the Creator of the universe, the LORD to provide me the chance to carry out my PhD and successfully completed the research study in Universiti Malaysia Sabah (UMS).

I would like to express my appreciation to my supervisor, Rosalam Hj. Sarbatly, a Professor in Chemical Engineering and the leader of Membrane Technology Research Group, Minerals and Materials Research Unit at UMS, for his consistent support and guidance throughout my PhD study.

Thanks to the financial supports of the Science Fund (SCF0055-AGR-2008) from the Ministry of Science and Technology Innovation Malaysia, the Exploratory Research Grant Scheme (ERG0001-TK-1/2011) and the MyBrain15 (MyPhD) scholarship from the Ministry of Higher Education Malaysia.

I also want to say 'thank you' to the lab assistants and technicians from Chemical Engineering Department and Mechanical Engineering Department for the help to complete the vacuum membrane distillation rig system including the circuit wiring and installing the instruments' holders. They are Mr. Abdullah Tarikim, Mr. Raysius Modi Atong, Mr. Yohanes Paulus Dua@Abdullah and Mr. Jasmi Jaya. For other technical lab works such as fixing the circuit wiring and fittings, I would like to convey my gratitude again to Mr. Abdullah Tarikim, Mr. Raysius Modi Atong and Mr. Freddy Disuk.

It is also worth to mention my friends who are doing research together and sharing the experience of research works with me.

Finally, I want to express my deepest gratefulness to my family for their support and enduring patience.

Chiam Chel Ken (詹秋景)

25 June 2014

ABSTRACT

This thesis presents a study of the heat and mass transfer performance in a laboratory-scale vacuum membrane distillation (VMD) process by using a rectangular cross-flow flat-sheet membrane module. One type of commercial polyvinylidene fluoride membrane with a nominal pore size of 0.2 μm and an effective area of 71.4 cm^2 is tested. Results show that the traditional Nusselt and Sherwood correlations, which are frequently employed in the membrane distillation literature, are not suitably used to estimate the heat and mass transfer coefficients in the VMD system for Reynolds numbers ranging from 150 to 1400. By using distilled water as the feed solution, a new semi-empirical heat transfer correlation by suggesting Knudsen-viscous mechanism governs the water vapour transport across the membrane is developed. Compared to the feed flow rate, the feed temperature is the limit to the heat transfer. The heat transfer coefficients are strongly dependent on the physical properties of the feed solution, but less relied on the design of the membrane module. A semi-empirical mass transfer correlation is derived based on the analogy between heat and mass transfer. In a desalination experiment, it was observed that approximately 30% of the experimental data fit well with the semi-empirical Nusselt and Sherwood correlations. The heat transfer process is limited by the resistances in the feed boundary layer and the membrane. The heat transfer resistance in the membrane increases when that in the feed boundary layer decreases and vice versa. More than 50% of the heat transfer resistances occur in the liquid feed phase at feed flow rates below 1200 mL/min, whereas the remaining occur in the membrane itself. At feed flow rates that exceed 1200 mL/min, the heat transfer resistance in the membrane becomes dominant. The Knudsen-viscous resistance controls the mass transfer through the membrane while the mass transfer resistance in the liquid feed phase is absent. The membrane deformed during the VMD operation as the result of the external pressure that originated from the hydraulic pressure of the feed solution and the vacuum pressure acts on the membrane downwardly. It was noticed that the dimples stamped on the membrane surface by the perforation of the support do not significantly affect the heat and mass transfer performance during VMD. The deformed membrane with the dimpled surface is compacted. The permeability of the deformed membrane is enhanced from 3 to 20% by the compaction as a result of the membrane thickness reduction. Nusselt and Sherwood correlations that consider membrane deformation are developed to predict the flux through the deformed membrane. The differences between the fluxes calculated using the correlations with membrane deformation effects and the correlations without membrane deformation effects are generally less than 9%, suggesting that membrane deformation due to the membrane permeability enhancement may exert no significant influence on the performance of VMD.

ABSTRAK

Pencirian Pemandahan Haba dan Jisim Dalam Membran Berlembaran-rata Berbentuk Segiempat untuk Penyulingan Membran Vakum

Tesis ini mengkaji pemandahan haba dan jisim bagi sebuah sistem penyulingan membran vakum (PMV) berskala makmal. Sistem PMV tersebut dikaji dengan menggunakan satu modul membran berlembaran-rata yang berbentuk segiempat. Sejenis membran komersial yang diperbuat daripada fluorida polivinilidene telah diuji. Membran tersebut mempunyai saiz liang nominal berukuran 0.2 μm . Keluasan membran yang digunakan adalah 71.4 cm^2 . Keputusan kajian menunjukkan bahawa korelasi-kolerasi Nusselt dan Sherwood tradisional, yang mana sering digunakan dalam kajian-kajian penyulingan membran, adalah tidak sesuai digunakan untuk menganggarkan pekali pemandahan haba dan jisim bagi sistem PMV dalam kajian ini yang beroperasi dalam lingkungan nombor Reynolds dari 150 hingga 1400. Satu kolerasi separa-empirik untuk pemandahan haba telah dibangunkan dengan menggunakan air suling sebagai suapan. Mekanisme Knudsen-likat menguasai pemandahan wap menerusi membran. Suhu suapan lebih mempengaruhi proses pemandahan haba jika dibandingkan dengan kadar aliran suapan. Pekali pemandahan haba adalah sangat bergantung kepada ciri-ciri fizikal larutan suapan tetapi ia kurang dipengaruhi oleh rekabentuk modul membran. Satu kolerasi separa-empirik untuk pemandahan jisim diperolehi berdasarkan analogi antara pemandahan haba dan jisim. Satu kajian penyahgaraman mendapati bahawa kira-kira 30% daripada data eksperimen menepati nilai-nilai yang dianggarkan dengan menggunakan korelasi-kolerasi separa-empirik Nusselt dan Sherwood tersebut. Rintangan dalam fasa suapan dan fasa membran menghadkan pemandahan haba. Pengaruh rintangan dalam fasa membran bertambah apabila rintangan dalam fasa suapan berkurang dan sebaliknya. Rintangan dalam fasa suapan mengawal lebih 50% daripada jumlah rintangan pemandahan haba apabila sistem PMV beroperasi kadar aliran suapan kurang dari 1200 mL/min. Rintangan dalam fasa membran menguasai proses pemandahan haba apabila kadar aliran suapan melebihi 1200 mL/min. Rintangan bermekanisme Knudsen-likat dalam fasa membran mengawal proses pemandahan jisim dalam PMV manakala rintangan pemandahan jisim dari fasa suapan boleh diabaikan. Permukaan dan struktur membran berubah bentuk kerana tekanan dari suapan dan tarikan vakum dikenakan pada membran semasa PMV beroperasi. Lekuk yang terbentuk pada permukaan membran tidak mempengaruhi proses pemandahan haba dan jisim, manakala ketelapan membran tersebut bertambah dari 3 hingga 20% yang disebabkan pepadatan di mana ketebalan membran berkurangan. Kolerasi-kolerasi Nusselt dan Sherwood telah dibangunkan dengan mempertimbangkan kesan membran berubah bentuk. Perbezaan antara fluks yang dianggarkan berdasarkan korelasi-kolerasi iaitu dengan mengambil kira kesan membran berubah bentuk dan tanpa kesan membran berubah bentuk adalah kurang daripada 9%, di mana kesan membran berubah bentuk boleh diabaikan.

TABLE OF CONTENTS

	Page
TITLE	i
DECLARATION	iii
CERTIFICATION	iv
ACKNOWLEDGEMENT	v
ABSTRACT	vi
<i>ABSTRAK</i>	vii
TABLE OF CONTENTS	viii
LIST OF TABLES	xii
LIST OF FIGURES	xv
LIST OF ABBREVIATIONS	xx
LIST OF SYMBOLS	xxi
LIST OF APPENDICES	xxv
CHAPTER 1: INTRODUCTION	1
1.1 Separation of Aqueous Solutions – An Overview	1
1.2 Membrane Distillation Configurations	4
1.2.1 Direct Contact Membrane Distillation	4
1.2.2 Air Gap Membrane Distillation	5
1.2.3 Sweeping Gas Membrane Distillation	6
1.2.4 Vacuum Membrane Distillation	6
1.3 Applications of Membrane Distillation	6
1.4 The Membranes	6
1.5 Feeding Techniques	8
1.6 Membrane Modules	10
1.7 Heat and Mass Transfer in MD	10
1.8 Benefits of the VMD	13
1.9 Problem Definition	14
1.9.1 Membrane Permeability	14

1.9.2	Process Conditions	15
1.9.3	Heat and Mass Transfer Coefficient	15
1.9.4	Membrane Deformation	16
1.10	Objectives	19
1.11	Outline of Thesis	19
CHAPTER 2: LITERATURE REVIEW		20
2.1	Introduction	20
2.2	VMD Process for Various Aqueous Solutions	20
2.3	Flat-sheet Membrane Modules	28
2.4	Heat Transfer	37
2.4.1	Heat Transfer across the Membrane	39
2.4.2	Heat Transfer on the Feed Side	40
2.5	Mass Transfer	42
2.5.1	Mass Transfer across the Membrane	44
2.5.2	Mass Transfer on the Feed Side	48
2.5.3	Experimental Mass Transfer Coefficient	51
2.6	Polarisations	53
2.6.1	Temperature Polarisation	53
2.6.2	Concentration Polarisation	55
2.6.3	Polarisation Profile	57
2.7	Membranes	57
2.7.1	Membrane Permeability	59
2.7.2	Membrane Wetting and Swelling	63
2.7.3	Commercial Membranes	65
2.8	Process Conditions	66
2.8.1	Feed Temperature	66
2.8.2	Feed Flow Rate	67
2.8.3	Feed Concentration	68
CHAPTER 3: THEORY AND METHODOLOGY		70
3.1	Introduction	70

3.2	Theoretical Investigation and Data Analysis	71
3.2.1	Measurement of Membrane Flux and Permeability	71
3.2.2	Measurement of Membrane Geometric Structure Parameter	74
3.2.3	Determination of Polarisation Coefficients	74
3.2.4	Development of Heat and Mass Transfer Models	83
3.2.5	Transport Resistances in Feed and Membrane Phases	88
3.3	Cross-flow VMD Experiment	88
3.3.1	Flat-sheet Membrane	88
3.3.2	Rectangular Membrane Module	88
3.3.3	Apparatus	91
3.3.4	Instrumentation	93
3.3.5	Calibration	93
3.3.6	Preparation of Feed Solutions	95
3.3.7	Process Conditions	95
3.3.8	Operation	95
3.3.9	Permeate Collection and Flux Determination	99
3.3.10	Feed Loss Analysis	101
3.3.11	Measurement of NaCl Concentration in Feed and Permeate	107
3.4	Low-pressure Gas Permeation Test	108
CHAPTER 4: RESULTS AND DISCUSSION		112
4.1	Introduction	112
4.2	Distilled Water VMD Experiment	113
4.2.1	Membrane Permeability	113
4.2.2	Performance of VMD	113
4.2.3	Temperature Polarisation Coefficient	118
4.2.4	Development of the Heat Transfer Correlation	118
4.2.5	Validation of Correlations	126
4.3	Desalination via VMD Experiments	130
4.3.1	Membrane Permeability	130
4.3.2	Performance of Desalination by VMD	130
4.3.3	Validation of Correlations	135

4.3.4	Equations of Heat and Mass Transfer Coefficients	139
4.3.5	Polarisation Effects	144
4.3.6	Transport Resistances	147
4.3.7	Heat Transfer Resistances in Feed and Membrane Phases	149
4.4	Influence of Membrane Deformation on the Performance of VMD	150
4.4.1	Membrane Deformation Induced by Perforated Support under the VMD Operation	150
4.4.2	Effect of Membrane Deformation on Membrane Permeability	153
4.4.3	Effect of Membrane Deformation on Heat and Mass Transfer Correlations	156
CHAPTER 5: CONCLUSIONS AND FUTURE WORK		162
5.1	Conclusions	162
5.1.1	Westran S Membrane Used in Pure Water Production via VMD	162
5.1.2	Development of Nusselt Correlation in Distilled Water VMD Experiments	162
5.1.3	Performance of Heat and Mass Transfer in Desalination via VMD	163
5.1.4	Influence of Membrane Deformation on the Performance of VMD	164
5.2	Suggestions for Future Work	165
5.2.1	Process Conditions	165
5.2.2	Temperature Measuring Probes	166
5.2.3	Designs of Membrane Module and Rig	166
5.2.4	Application of the Developed Heat and Mass Transfer Correlations	167
REFERENCES		168
APPENDICES		183
LIST OF PUBLICATIONS		212

LIST OF TABLES

	Page
Table 1.1: Driving forces distinguish the membrane processes (Koros <i>et al.</i> , 1996)	2
Table 1.2: Overview of potential applications of membrane distillation in various industries	7
Table 2.1: Single component transport process of desalination	26
Table 2.2: Single component transport process of concentration	27
Table 2.3: Binary component transport process of organic compound extractions	29
Table 2.4: Binary component transport process of dissolved gas removals	30
Table 2.5: Multicomponent transport process of aroma compound separations	31
Table 2.6: Commercial flat-sheet membranes commonly used in VMD (membrane thickness: δ ; mean pore size: d_p ; porosity: ε ; tortuosity: τ ; membrane permeability coefficient: k_m)	34
Table 2.7: Feed liquid phase heat transfer correlations for VMD systems in literature	41
Table 2.8: Feed liquid phase mass transfer correlations for VMD systems in literature	50
Table 2.9: Membrane permeability values at the corresponding fluxes (Chiam and Sarbatly, 2013)	64
Table 3.1: Summary of the correlations commonly used for the estimation of heat transfer in feed flow channels under laminar flow	77
Table 3.2: Summary of the analogous Sherwood correlations used for feed flow channels under laminar flow	81
Table 3.3: Properties of the Westran S membrane provided by the manufacturer	89

Table 3.4:	Calibration of heating bath and temperature transmitters after 30 minutes	96
Table 3.5:	The process conditions of the VMD separation experiments	96
Table 3.6:	The mean values of water vapour loss for various feed temperatures	105
Table 4.1:	b values from of Equation (3.29) using a log-log plot of Nu versus Re	122
Table 4.2:	Values of c and a , from fits of Equation (3.29) using a log-log plot of the factor (Nu/Re^b) versus Pr	123
Table 4.3:	Selected heat and mass transfer coefficient equations for feed bulk temperature ranging from 65 to 80°C	145
Table 4.4:	Values of a , b and c from fits of Equation (3.29) using log-log plots of (Nu) versus (Re) and (Nu/Re^b) versus (Pr)	160
Table A.1:	Viscosity of liquid water	185
Table A.2:	Thermal conductivity of liquid water	187
Table C.1:	Collection of permeate through the Westran S membrane with area of 71.4 cm ² for 10 minutes when distilled water is tested as the feed solution	191
Table C.2:	Collection of permeate through the Westran S membrane with area of 71.4 cm ² for 10 minutes when 2.0 wt% NaCl solution is tested as the feed solution	192
Table C.3:	Collection of permeate through the Westran S membrane with area of 71.4 cm ² for 10 minutes when NaCl solutions are tested as the feed solutions at temperature of 80°C	192
Table D.1:	The time (t in second unit) taken of a soap film rises 20 cm in the acrylic pipe at various pressure differences (ΔP) across the membranes in undeformed state	194
Table D.2:	The time (t in second unit) taken of a soap film rises 20 cm in the acrylic pipe at various pressure differences (ΔP) across the membranes in deformed state after distilled water VMD experiments	195
Table D.3:	The time (t in second unit) taken of a soap film rises 20 cm in the acrylic pipe at various pressure differences (ΔP) across the membranes in deformed state after 2.0 wt% NaCl solution VMD experiments at 80°C	198

Table D.4:	The time (t in second unit) taken of a soap film rises 20 cm in the acrylic pipe at various pressure differences (ΔP) across the membranes in deformed state after 0.5 – 2.0 wt% NaCl solution VMD experiments	200
Table E.1:	Example of experimental conditions	204
Table E.2:	Example of experimental conditions	208



UMS
UNIVERSITI MALAYSIA SABAH

LIST OF FIGURES

	Page
Figure 1.1: Different types of MD configurations (Lawson and Lloyd, 1997; El-Bourawi <i>et al.</i> , 2006); (a) DCMD, (b) AGMD, (c) SGMD, and (d) VMD.	5
Figure 1.2: Feeding techniques of membrane distillation systems (Koros <i>et al.</i> , 1996). (a) Dead-end system and (b) cross-flow system.	9
Figure 1.3: The heat and mass transfer in MD process (Schofield <i>et al.</i> , 1987; Gryta and Tomasweska, 1998; El-Bourawi <i>et al.</i> , 2006).	11
Figure 1.4: Hypothesised polarisation layer formation on (a) an impermeable and rigid solid; (b) a permeable and porous solid. (Ramon <i>et al.</i> , 2009; Chiam and Sarbatly, 2014)	17
Figure 2.1: The principle of VMD separation process (Bandini <i>et al.</i> , 1997; Qi <i>et al.</i> , 2012; Dao <i>et al.</i> , 2013).	21
Figure 2.2: The groups of VMD separation processes based on different applications (Chiam and Sarbatly, 2013).	24
Figure 2.3: Schematic of the flat-sheet membrane module. (a) – (f): Laboratory-scale; (g) – (h): Commercial-scale.	36
Figure 2.4: Heat transfer resistances in membrane distillation (Schofield <i>et al.</i> , 1990; Khayet <i>et al.</i> , 2000).	38
Figure 2.5: Mass transfer resistances in membrane distillation (Lawson and Lloyd, 1997; Khayet, 2011).	43
Figure 2.6: A generic schematic diagram of the VMD system (Wang <i>et al.</i> , 2009a; Qi <i>et al.</i> , 2012).	52
Figure 2.7: Polarisation profiles in VMD (Chiam and Sarbatly, 2013): (a) no temperature and concentration polarisations, (b) temperature polarisation, (c) concentration polarisation, and (d) temperature and concentration polarisations.	58
Figure 2.8: Partial pressure drops over the aqueous feed liquid phase and the porous membrane (Chiam and Sarbatly, 2013).	62

Figure 3.1:	Hypothetical diagram of the heat and mass transfer in the cross-flow VMD process (Bandini and Sarti, 1999; Criscuoli <i>et al.</i> , 2008).	75
Figure 3.2:	Figure 3.2: SEM images of the Westran S membrane for (a) top surface (4000 ×); (b) cross-section (1000 ×); and (c) bottom surface (5000 ×).	89
Figure 3.3:	Cross- sectional view of the rectangular cross-flow flat-sheet membrane module in scale 1:1.	90
Figure 3.4:	Schematic diagrams of physical flow of the experimental VMD apparatus. 1: module with a flat membrane; 2: feed reservoir; 3: feed pump; 4: rotameter; 5: temperature control bath with heating coil; 6: cold trap housed in dewar; 7: temperature transmitters; 8: pressure gauges; 9: vacuum pump; 10: feed valve; 11: retentate discharging valve; 12: beaker for retentate collection; 13: vent valve; and 14: standby valve.	92
Figure 3.5:	The calibration curve of the digital gear pump. The intercept value of -0.6612 g/s is due to moving air at the surrounding that affecting the displayed reading on the electronic balance becomes non-zero.	94
Figure 3.6:	Variation of measured temperature with preheating time at 70 and 90°C in the water bath and the module inlet.	98
Figure 3.7:	A comparison of the inlet module temperature and water bath temperature at around 5 th and 9.5 th minute during VMD operation as well as the 1-h preheating temperature.	100
Figure 3.8:	Retentate discharging and collected into the beaker at the end of each VMD experimental run.	102
Figure 3.9:	Vapour loss versus time for water depths 2 and 14 cm in the beaker at various feed temperatures.	104
Figure 3.10:	Determination of the mass flow rate of the retentate discharging. The intercept value of 149.05 g is because the electronic balance displayed non-zero when the recording of the weight is started.	106
Figure 3.11:	The calibration curve of concentration versus conductivity of NaCl solution.	109
Figure 3.12:	Low-pressure gas permeation test for membrane permeability measurement (not to scale). 1: module with a flat membrane; 2: acrylic pipe; 3: N ₂ gas reservoir; 4: digital	110

manometer; 5: needle valve; 6: soap solution; 7: a thin soap film and 8: ball (drain) valve.

Figure 4.1:	The measurement of membrane permeability reported as N ₂ gas flux versus the gas pressure difference for five samples of Westran S membrane. The solid lines are the Knudsen diffusion fits of the data.	114
Figure 4.2:	Experimental flux (J_{exp}) as function of the feed flow rate (Q_f) for different feed temperatures for distilled water as the feed solution.	115
Figure 4.3:	Experimental flux (J_{exp}) as function of the feed temperature (T_f) for different feed flow rate for distilled water as the feed solution. The solid lines are the Arrhenius fits of the data, $J \propto \exp(-\Delta H_v/RT_f)$.	117
Figure 4.4:	Variation of TPC with feed flow rate (bottom scale) at 85°C and with feed temperature (top scale) at 900 mL/min of distilled water as the feed solution.	119
Figure 4.5:	$\log(Nu)$ versus $\log(Re)$ for the respective constant feed temperatures from 75 to 95°C. The solid lines are linear least squares fits of the experimental data.	121
Figure 4.6:	$\log(Nu/Re^{0.97})$ versus $\log(Pr)$ for feed temperature from 75 to 95°C and feed flow rate from 450 to 1200 mL/min. The solid line is linear least squares fit of the experimental data. The dashed lines represent 97% of confidence interval.	124
Figure 4.7:	Plots of the Nusselt numbers (Nu) versus the Reynolds numbers (Re) for both the experimental data and the correlations. The traditional correlations (1) – (4) are listed in Table 3.1.	127
Figure 4.8:	The comparison of the experimental heat transfer coefficients (h_{exp}) with the heat transfer coefficients calculated (h_{cal}) by the correlation developed in this study.	129
Figure 4.9:	The comparison of the experimental fluxes (J_{exp}) with the fluxes calculated (J_{cal}) by the correlation developed in this study.	131
Figure 4.10:	Experimental flux (J_{exp}) as a function of the feed flow rate (Q_f) at different feed temperatures using 2.0 wt% NaCl solution as the feed solution.	133
Figure 4.11:	Experimental flux (J_{exp}) as a function of the feed	134

temperature (T_f) at different feed flow rates using 2.0 wt% NaCl solution as the feed solution. The solid lines are the Arrhenius fits of the data, $J \propto \exp(-\Delta H_v/RT_f)$.

- Figure 4.12: Experimental flux (J_{exp}) as a function of the feed flow rate (Q_f) at different feed concentrations and a constant feed temperature of 80°C. 136
- Figure 4.13: Experimental flux (J_{exp}) as a function of the feed concentration (C_f) at different feed flow rates and a constant feed temperature of 80°C. 137
- Figure 4.14: A comparison of the experimental fluxes (J_{exp}) and the fluxes calculated (J_{cal}) by the correlations. The traditional correlations (1) – (4) are listed in Tables 3.1 and 3.2. 138
- Figure 4.15: The good agreement between 30% of the experimental fluxes (< 30 kg/m² h) and the fluxes calculated by the correlations derived in Equation (4.1). 140
- Figure 4.16: Relationship between transport coefficients and feed bulk temperature (65 – 80°C) for feed flow rates ranging from 300 to 1800 mL/min and feed concentrations ranging from 0.5 to 4.0 wt% NaCl. 142
- Figure 4.17: Temperature and concentration polarisation coefficients for feed flow rates ranging from 300 to 1800 mL/min, feed temperatures ranging from 65 to 80°C and feed concentrations ranging from 0.5 to 4.0 wt% NaCl. 146
- Figure 4.18: Feed boundary layer resistance and membrane resistance for feed flow rates ranging from 300 to 1800 mL/min, feed temperatures ranging from 70 to 80°C and feed concentrations ranging from 0.5 to 4.0 wt% NaCl. 148
- Figure 4.19: Heat transfer resistances in the feed boundary layer and the membrane for feed flow rates ranging from 300 to 1800 mL/min, feed temperatures ranging from 70 to 80°C and feed concentrations ranging from 0.5 to 4.0 wt% NaCl. 151
- Figure 4.20: Perforated support induced membrane deformation under the VMD operation. (a) Images of the perforated aluminium support and the polymeric membrane after subjected in the VMD experiments; (b) a schematic representation of the polymeric membrane in the undeformed state and deformed state. 152
- Figure 4.21: Changes of the permeability of a Westran S membrane 154

sample subjected to the VMD operation for various feed temperatures under a feed flow rate of 600 mL/min.

- Figure 4.22: Membrane permeability enhancement due to membrane deformation and compaction after tested in the VMD operation at various feed temperatures under respective constant feed flow rates. 157
- Figure 4.23: Development of the Nusselt correlation by considering the membrane permeability enhancement due to membrane deformation and compaction. (a) $\log(Nu)$ versus $\log(Re)$ for the respective constant feed temperatures from 75 to 95°C. The solid lines are linear least squares fits of the experimental data. (b) $\log(Nu/Re^{0.95})$ versus $\log(Pr)$ for feed temperature from 75 to 95°C and feed flow rate from 450 to 1200 mL/min. The solid line is linear least squares fit of the experimental data. The dashed lines represent 97% of confidence interval. 159
- Figure 4.24: A comparison of the experimental fluxes and the fluxes calculated by the correlations. (a) Distilled water is feed solution; (b) NaCl solutions are the feed solutions. 161
- Figure B.1: The lab-fabricated VMD system employed in this work 189
- Figure B.2: Lab-fabricated low pressure gas permeation system 190



UMS
UNIVERSITI MALAYSIA SABAH

LIST OF ABBREVIATIONS

AGMD	-	Air gap membrane distillation
CPC	-	Concentration polarisation coefficient
DCMD	-	Direct contact membrane distillation
DW	-	Distilled water
LEP_w	-	Liquid entry pressure of water
V-L	-	Vapour-liquid
MD	-	Membrane distillation
MDE	-	Membrane deformation effect
MTBE	-	methyl tert-butyl ether
NaCl	-	Sodium chloride
PE	-	Polyethylene
PP	-	Polypropylene
PTFE	-	Polytetrafluoroethylene
PV	-	Pervaporation
PVDF	-	Polyvinylidene fluoride
PVP	-	Polyvinylpyrrolidone
RO	-	Reverse osmosis
SEM	-	Scanning electron microscopy
SGMD	-	Sweeping gas membrane distillation
SMS	-	Smooth membrane surface
TCA	-	1,1,1-trichloroethane
TCE	-	trichloroethylene
TPC	-	Temperature polarisation coefficient
VLE	-	Vapour-liquid equilibrium
VMD	-	Vacuum membrane distillation
VOC	-	Volatile organic compound

LIST OF SYMBOLS

a	- Empirical constant for Equation (3.29)
A	- Area (m^2)
c	- Concentration (mol/m^3)
C	- Membrane distillation coefficient, mass transfer coefficient ($kg/m^2 s Pa$)
C_p	- Heat capacity ($J/kg K$)
d	- Diameter (m)
D	- Diffusion coefficient (m^2/s)
F_c	- Tube-row correction factor (-)
g	- Gravitation acceleration ($9.81 m/s^2$)
Gr	- Grashof number (-)
Gz	- Graetz number (-)
h	- Individual heat transfer coefficient ($W/m^2 K$)
H	- Overall heat transfer coefficient ($W/m^2 K$); Henry's constant (Pa)
ΔH_v	- Heat of vaporisation (J/kg)
J	- Mass flux ($kg/m^2 s$ or $kg/m^2 h$)
k	- Individual mass transfer coefficient ($kg m/mol s$ or m/s); thermal conductivity ($W/m K$)
k_B	- Boltzmann constant ($1.38 \times 10^{-23} J/K$)
kn	- Knudsen number (-)
K_m	- Membrane permeability coefficient ($s mole^{1/2} m^{-1} kg^{-1/2}$)
K	- Overall mass transfer coefficient ($W/m K$)
L	- Length (m)
m	- Mass (kg)
M	- Molecular weight (kg/mol)
n_s	- Mole fraction of solute (-)
n_+, n_-	- Valence (-)
Nu	- Nusselt number (-)
p	- Partial pressure (Pa)

P	- Vapour pressure, absolute pressure (Pa)
\bar{P}	- Mean partial pressure (Pa)
P°	- Saturation vapour pressure (Pa)
Pr	- Prandtl number (-)
Q	- Heat flux ($\text{J}/\text{m}^2 \text{ s}$)
r	- Radius (m)
R	- Resistance ($\text{m}^2 \text{ s K}/\text{J}$ or $\text{m}^2 \text{ s Pa}/\text{kg}$); rejection (%); universal gas constant ($8.31 \text{ J}/\text{mol K}$)
R_v	- Removal efficiency (%)
Re	- Reynolds number (-)
s	- Standard deviation ($\text{kg}/\text{m}^2 \text{ s}$)
s_w	- Minimum weighed standard deviation (-)
Sc	- Schmidt number (-)
Sh	- Sherwood number (-)
t	- Time (s)
T	- Temperature (K)
v	- Diffusion volume (m^3); velocity (m/s)
V	- Volume (m^3)
w	- Weight (kg)
\dot{w}	- Rate of water vapour lost (kg/s)
x	- Mass fraction (-)
y	- Mole fraction in vapour phase (-)

Subscript

0	- Initial
1	- Final, upstream
2	- Downstream
A	- Component A
b	- Bulk
B	- Component B
c	- Cold
cal	- Calculated

d	-	One drop
dis	-	Discharging
e	-	Exposed
exp	-	Experimental
f	-	Feed
G	-	Gas
h	-	Hot; hydraulic
<i>i, j</i>	-	Component <i>i, j</i>
I	-	Interface
Kn	-	Knudsen-type
L	-	Liquid
m	-	Membrane
op	-	Operation
p	-	Permeate; pore
percen.	-	Percentage (%)
r	-	Retentate
s	-	Solid; smooth
T	-	Total
U-D	-	Upstream to downstream
v	-	Vaporisation; vapour
vis	-	Viscous-type
w	-	Water

Superscript

<i>b, c</i>	-	Empirical constants for Equation (3.29)
HT	-	Heat transfer
MT	-	Mass transfer
*	-	Equilibrium

Greek letter

α	-	Separation factor (-)
β	-	Concentration factor (-); thermal expansion coefficient (K^{-1})

- γ - Surface tension (N/m); activity coefficient (-)
- δ - Thickness (m)
- ε - Porosity (-)
- η_v - Viscosity of vapour (Pa s)
- θ - Angle ($^\circ$)
- λ - Mean free path (m)
- λ_+, λ_- - Limiting ionic conductance (-)
- μ - Viscosity of liquid (Pa s)
- ρ - Density (kg/m^3)
- σ - Collisions diameter (m)
- τ - Tortuosity (-)



UMS
UNIVERSITI MALAYSIA SABAH